OFFICE OF NAVAL RESEARCH

Contract ~~N0014-79-C-0012~~ N00014-79-C

Task No. 12139

TECHNICAL REPORT NO. 11

PLASMA POLING OF POLY(VINYLIDENE FLUORIDE): PIEZO- AND PYROELECTRIC RESPONSE

by

J. E. McKinney, G. T. Davis, and M. G. Broadhurst

Prepared for Publication

in the

Journal of Applied Physics

National Bureau of Standards
Polymer Science & Standards Division
Washington, D.C. 20234

June, 1979

DISCLAIMER NOTICE

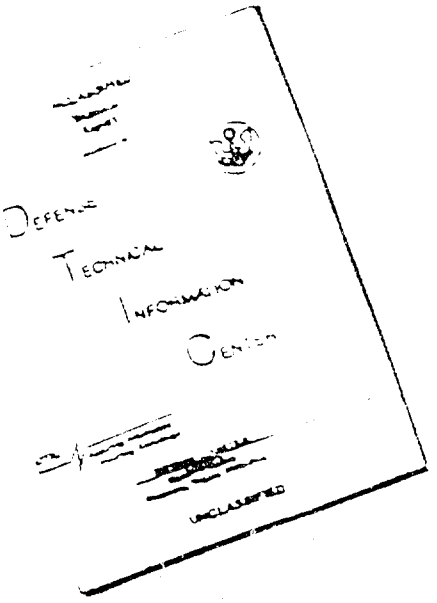

THIS DOCUMENT IS BEST QUALITY AVAILABLE. THE COPY FURNISHED TO DTIC CONTAINED A SIGNIFICANT NUMBER OF PAGES WHICH DO NOT REPRODUCE LEGIBLY.

SECURITY CLASSIFICATION OF THIS PAGE (When Data Entered)

REPORT DOCUMENTATION PAGE

READ INSTRUCTIONS BEFORE COMPLETING FORM

1. REPORT NUMBER: Technical Report # 11
2. GOVT ACCESSION NO.
3. RECIPIENT'S CATALOG NUMBER

4. TITLE (and Subtitle): PLASMA POLING OF POLY(VINYLIDENE FLUORIDE): PIEZO- AND PYROELECTRIC RESPONSE

5. TYPE OF REPORT & PERIOD COVERED: Technical Report # 11

6. PERFORMING ORG. REPORT NUMBER

7. AUTHOR(s): J. E. McKinney, G. T. Davis, M. G. Broadhurst

8. CONTRACT OR GRANT NUMBER(s): N0014-79-C-0012

9. PERFORMING ORGANIZATION NAME AND ADDRESS
National Bureau of Standards
Polymer Science & Standards Division
Washington, D.C. 20234

10. PROGRAM ELEMENT, PROJECT, TASK AREA & WORK UNIT NUMBERS
Task No. NR 212139

11. CONTROLLING OFFICE NAME AND ADDRESS
Office of Naval Research
Chemistry Program
Arlington, VA 22217

12. REPORT DATE: June 1979

13. NUMBER OF PAGES: 25

14. MONITORING AGENCY NAME & ADDRESS (if different from Controlling Office)

15. SECURITY CLASS. (of this report): Unclassified

15a. DECLASSIFICATION/DOWNGRADING SCHEDULE

16. DISTRIBUTION STATEMENT (of this Report)

According to attached distribution list.

This document has been approved for public release and sale; its distribution is unlimited.

17. DISTRIBUTION STATEMENT (of the abstract entered in Block 20, if different from Report)

18. SUPPLEMENTARY NOTES

To be published in Journal of Applied Physics

19. KEY WORDS (Continue on reverse side if necessary and identify by block number)

Charge; compressibility; piezoelectricity; plasma; polarization; poly(vinylidene flurodie); pyroelectricity; thermal expansion.

20. ABSTRACT (Continue on reverse side if necessary and identify by block number)

A plasma poling technique and its use with polyvinylidene fluoride (PVDF) films is described. Specimens of biaxially drawn (blow extruded) PVDF containing both Form I (β) and Form II (α) crystals were poled under various conditions in a plasma field while the charging current was monitored to determine the polarization. Subsequently, both piezo- and pyroelectric activity were measured in order to evaluate their magnitudes with respect to the remnant polarization (that is, the polarization remaining after

DD FORM 1 JAN 73 1473 EDITION OF 1 NOV 68 IS OBSOLETE
S/N 0102-014-6601

SECURITY CLASSIFICATION OF THIS PAGE (When Data Entered)

Block 20 - continued

returning the applied field to zero). The results are shown to be in reasonable quantitative agreement with the predictions of a model of PVDF consisting of a mixture of preferentially aligned crystals in randomized amorphous material.

PLASMA POLING OF POLY(VINYLIDENE FLUORIDE): PIEZO-AND PYROELECTRIC RESPONSE

J. E. McKINNEY, G. T. DAVIS, M. G. BROADHURST

NATIONAL BUREAU OF STANDARDS

WASHINGTON, D.C. 20234

ABSTRACT

A plasma poling technique and its use with polyvinylidene fluoride (PVDF) films is described. Specimens of biaxially drawn (blow extruded) PVDF containing both Form I (β) and Form II (α) crystals were poled under various conditions in a plasma field while the charging current was monitored to determine the polarization. Subsequently, both piezo- and pyroelectric activity were measured in order to evaluate their magnitudes with respect to the remnant polarization (that is, the polarization remaining after returning the applied field to zero). The results are shown to be in reasonable quantitative agreement with the predictions of a model of PVDF consisting of a mixture of preferentially aligned crystals in randomized amorphous material.

INTRODUCTION

Polyvinylidene fluoride (PVDF) is a unique transducer material because of its toughness, flexibility, low density, low mechanical impedance and ease of fabrication. To achieve optimum performance from this material, one would like to have a broad understanding of mechanisms underlying its activity. In previous papers we have shown evidence that application of large electric fields to PVDF films reorients molecular dipoles in the crystal phase [1] and that the response to thermally or mechanically induced strains of preferentially oriented, polar crystals of PVDF can account quantitatively for the piezoelectric and pyroelectric activity of PVDF films.[2] In this paper we report the results of some poling experiments [3] where we measured the remnant polarization (that is, the polarization remaining after returning the applied field to zero)resulting from application of large electric fields and show the relationship between this polarization and pyroelectric data. This comparison further supports a model where oriented polar crystals are the basis of the transducer effects in PVDF.

Day and coworkers [4] carried out systematic studies with 6 μm biaxially oriented PVDF films for a variety of polarization conditions (time, electric field intensity and temperature) and measured the resultant pyroelectric activity. They concluded that activity increased with the intensity and duration of the polarizing field, and with the polarizing temperature. They also found that the activity becomes more uniform across the film thickness at longer times and higher fields and temperature. When non-uniform, the activity was greatest at the side of the film which was positive during polarization, in accord with other reports[5-7].

Southgate poled PVDF at room temperature and measured both the remnant polarization and pyroelectric coefficient, using a corona poling method [8]. Of the films used (9 to 16 μm thick), the largest effects were observed with the thinnest films. Southgate's data showed that the pyroelectric coefficient increases roughly proportional to the remnant polarization and that the

polarization increases with the magnitude of the poling field. He reported polarizations as high as 9 $\mu C/cm^2$ which represents about 75% of the maximum polarization obtainable with a 60% crystalline (Form I) specimen. (The calculated single crystal polarization for Form I is about 20 $\mu C/cm^2$ if one includes enhancement of the vacuum moment by the reaction field of the solid surroundings).

The pyroelectric activity of PVDF was studied by Blevin [9] as a function of poling time and temperature using 6 μm thick films and a poling field of 1 MV/cm. Blevin concluded that the pyroelectric coefficient increases faster at higher poling temperatures and further that the ultimate polarization depends only on the electric field and does not depend on poling temperature.

Poling of 40 to 200 μm thick films of PVDF was achieved by Tamura and coworkers [10] over a wide temperature range. They found the remnant polarization decreases with poling temperature from maximum values at room temperature to zero near the glass transition temperature (-40° C). These results suggest that orientation of the polar crystal segments is facilitated by mobility in the intercrystalline amorphous phase. Tamura et. al, showed that well formed hysteresis curves could be obtained with PVDF by measuring the charge on the electrodes due to a sinusoidally varying voltage. The critical field for developing a remnant polarization was found to decrease with an increase in temperature. We suppose from the above discussion of time effects that the magnitude of the field needed to produce a given remnant polarization increases with increasing frequency also. That is, we expect the hysteresis loop to close with increasing frequency.

Similar hysteresis curves have been reported by Kepler [11] and observed in our laboratory. Oshiki and Fukada [12] have published a hysteresis curve for the piezoelectric stress-coefficient e_{31} vs applied field. We expect this curve to closely follow the polarization-field hysteresis curves though detailed comparisons of this kind have yet to be reported.

Murayama and co-workers [13] studied piezoelectricity in uniaxially oriented β phase PVDF polarized at temperatures from 25°C to 110°C and they reported d_{31} was proportional to polarizing field without the threshold field expected from the hysteresis results.

The connection between polarization in PVDF and reorientation of molecular dipoles in the crystal phase is becoming documented with IR [1,8,10, 14-18] and x-ray [1,3,15,19-22] data. Field-induced conversion from Form II to polar Form II and at still higher fields to Form I has also been demonstrated [1,8,15,20]. This latter transformation involves not only reorientation of molecular segments in the crystal phase but also changes in conformation from $tgtg'$ to all trans.

With the strong evidence for field-induced reorientation of molecular dipoles in the crystal phase of PVDF and the availability of a theoretical model for the piezoelectric and pyroelectric response we can now test the model with a more complete set of data as presented in this paper.

II. Theoretical Considerations

We assume that polar crystal lamellae in a film of PVDF become preferentially aligned normal to the plane of the film by the action of a large applied field. The material is conductive enough (resistivity $\sim 10^{15}\Omega$-cm) that ionic charges are assumed to be mobile in the presense of internal fields during poling and storage of the films. A possible depoling process involving ionic mobility is depicted schematically in Fig. 1, where the ionic charges are shown to move to the crystal surfaces producing a decrease in the polarization with time. Although the polarization may completely vanish as shown (if sufficient carriers are available), the piezoelectric and pyroelectric coefficients (d_p and p_y) do not. This is because the moments due to charges and those due to dipoles change differently with changes in temperature and pressure. The theory developed from this model

by Broadhurst and co-workers [2] gives the following expression for the surface charge, Q_s, on the short circuited conductive electrodes on the PVDF film:

$$Q_s = [(1/3)N(\varepsilon_c + 2)\mu_0 J_0(\phi_0) + Q\ell_c] \langle \cos \theta_0 \rangle / \ell_s \qquad (1)$$

where N is the total number of dipoles, ε_c is the relative permittivity of the polymer crystal, μ_0 is the amount of repeat unit in vacuum, J_0 is the Bessel function of order zero of the libration amplitude ϕ_0, ℓ_s is the sample thickness or electrod3 separation, Q is the total countercharge separated by the mean crystal length, ℓ_c, and θ_0 is the angle between the crystal moment and the axis normal to the film surface.

The change in electrode charge with applied mechanical or thermal stress is found by taking the derivatives of eq. (1) with respect to that stress. The experimental hydrostatic piezoelectric coefficient $d_p = A^{-1}\, dQ/dp$ and pyroelectric coefficient, $p_y = A^{-1} dQ/dT$, where A is the electrode area, are given by:

$$d_p = P_0 \beta_c [1/3(\varepsilon_c - 1) + \phi_0^2 \gamma + r(\partial \ln \ell_c / \partial \ln V_c)_T + (1-r)(\partial \ln \ell_s / \partial \ln V_c)_T] \qquad (2a)$$

$$p_y = -P_0 \alpha_c [1/3(\varepsilon_c - 1) + \phi_0^2 (\gamma + (2T\alpha_c)^{-1}) + r(\partial \ln \ell_c / \partial \ln V_c) + (1-r)(\partial \ln \ell_s / \partial \ln V_c)_T] \qquad (2b)$$

where $P_0 = 1/3\, \Phi(\varepsilon_c + 2)\, N\mu_0 J_0(\phi_0) \langle \cos \theta_0 \rangle / V_c \qquad (3)$

is the remnant polarization obtained immediately after poling, Φ is the volume fraction crystallinity, β_c and α_c are the crystal compressibility and thermal expansion, γ is the Gruneisen constant $(-\partial \ln \omega / \partial \ln V_c)_p$, where ω is the libration frequency; p is pressure; T is temperature; V_c is the crystal volume and the polarization from the countercharge is assumed to be some fraction r between 0 and 1 of that from the dipoles. Eqs. (2) have been made explicit by letting

$$Q = (1/3)\, rN(\varepsilon_c + 2)\mu_0 J_0(\phi_0)/\ell_c \qquad (4)$$

The term ϕ_0^2 in eqs (2) results from the approximation $\phi_0 = 2\, J_1(\phi_0)/J_0(\phi_0)$ where J_1 is a first order Bessel function. Eqs (2) can be evaluated over the range from no countercharge ($r = 0$) to complete countercharge ($r = 1$).

In evaluating the derivatives involving ε_c in eqs (2) we have assumed that expansions along the polymer backbone are negligible (in both α and β phases). Thus the corresponding linear expansions from temperature and pressure changes are $\alpha_c/2$ and $\beta_c/2$ for which

$$(\partial \ln \varepsilon_c / \partial \ln V_c)_T = (\partial \ln \varepsilon_c / \partial \ln V_c)_p = 1/2$$

Similarily, for the derivative involving ε_s, we have assumed linear expansions corresponding to $\alpha_s/2$ and $\beta_s/2$. Thus:

$$(\partial \ln \varepsilon_s / \partial \ln V_c)_T = \beta_s/2\beta_c \tag{5a}$$

$$(\partial \ln \varepsilon_s / \partial \ln V_c)_p = \alpha_s/2\alpha_c \tag{5b}$$

Eqs (2) can be evaluated for either Form I, polar Form II or mixtures of the two if the volume fractions, and expansion data are known. Recently, x-ray compressibilities have become available for both Form I and Form II crystals [24].

For Form II PVDF, using the values $\alpha_s = 4.2 \times 10^{-4}$ K^{-1}, $\alpha_c = 1.7 \times 10^{-4}$, $\beta_s = 2.39 \times 10^{-11}$ Pa^{-1} and $\beta_c = 1.1 \times 10^{-11}$ from Table 1 of Ref. 2, we obtain 1.09 and 1.24 for the values of the derivatives given by eq. (5a) and (5b), respectively. Not all of the corresponding physical constants for form I are available but one might expect the values of ratios in Eqs. 5 to be similar for different forms of the same polymer.

Experimental

The chamber used to generate plasma for the poling process was adapted from a commercial plasma cleaner. The electrode assembly, mounted on the face plate, is shown schematically in Fig. 2. It was made of polystryene because of its apparent durability and superior electrical properties. An aluminum electrode 2.5 cm in diameter is evaporated on one side of the 25 μm thick polymer film. The sample is clamped as shown with the non-metallized side exposed to the plasma. The purpose of the aluminum electrode is to insure homogeneous electrical contact with the electrode assembly. The chamber (containing air) is

evacuated to, and maintained at, about 200 mT for the poling process. Water vapor and other condensable gases are removed with a liquid nitrogen trap.

Voltages up to 10 kV may be applied across the plasma generator between the electrodes as shown in Fig. 3. It is assumed that essentially all of the potential drop from the grounded grid to the high potential evaporated electrode occurs across the specimen because of the high conductivity of the plasma relative to the specimen. The charge transfer is measured with a charge amplifier in series with the high voltage power supply as shown schematically in Fig. 3. The amount of charge is a measure of the polarization during the poling process and the remnant polarization which remains after removal of the electric field. The polarity of the high voltage supply produces a positively charged plasma as shown in Fig. 3. When the polarity was reversed there was no apparent influence on the magnitude of polarization. The effect of electrical leakage on the determination of polarization was found to be negligible over the short poling times used. In this work the applied field is taken as the average field, which is the applied voltage shown in Fig. 3 divided by the specimen thickness.

After the specimen is poled, a graphite electrode (from colloidal graphite in water) is painted on the non-metallized side of each specimen. The electrodes are shorted, and the specimens are stored for at least 12 hours to stabilize discharge currents which come from the specimen. The piezoelectric coefficient d_p is then measured in a pressure cell [23] employing a current amplifier and imposing nearly constant rates of pressure change (both pressurization and depressurization). From the slopes of the pressure-time curves and the corresponding current, d_p is determined. In an analogous manner the pyroelectric current resulting from nearly constant rates of temperature change (both heating and cooling) is measured using the same cell in the neighborhood of room temperature. To reduce the effects of temperature and pressure dependent background currents, we used the difference between the current for rising pressure or temperature and that for falling pressure or temperature measured at the same pressure or temperature. The response measured

in this way included only reversible currents and is independent of background currents such as the release of stored charge following poling, and currents resulting from electrode-polymer reactions. Thermally stimulated currents are not present during the measurements since the temperature cycling is done at temperatures near the storage temperature of the films.

RESULTS

The remnant polarization is a consequence of irreversible response manifested by hysteresis loops of the kind shown of Fig. 4, where the polarization P, is plotted against the applied field, E. This data was obtained by manually varying the voltage between -5 and 5 kV at essentially constant rates approximating ± 500 V/s. At the ordinate crossovers the power supply terminals were reversed rapidly such that significant relaxations were not possible. As mentioned earlier the polarization is determined from the measurement of the charge transfer. With the rate given above, the leakage current has an insignificant effect. Initially, the response is very unstable, as indicated, and often breakdown occurs prematurely at low fields. After the first cycle, however, the response is very smooth, symmetrical, and reproducible (but not reversible) even though there are some small variations in the rates at which the voltage is changed. In this case the applied field is not high enough to reach saturation, however, the response appears to begin to level off at the high fields.

In order to obtain a more quantitative evaluation of the quantities to be determined, the specimens were poled using step function fields at various levels. The total charge transfer is measured by the integrating circuit mentioned earlier. The leakage current may be determined by measuring the slope of the charge-time curves at large times where the response is essentially linear with time. Fig. 5 illustrates an example of these results where the polarization at 5 kV is plotted as a function of time. The value of the remnant polarization P_0 is taken as the apparent steady state after the removal of the applied field. Although it

is mentioned earlier in this paper that P may relax, or even vanish, as a consequence of real charge transfer to the crystal-liquid interfaces, these relaxation times are much longer than the time scale of Fig. 5. The straight line with small positive slope at the bottom of the figure corresponds to the leakage current from which the value of resistivity $\rho = 6.2 \times 10^{14}$ Ω - cm is obtained. The corresponding leakage charge was subtracted from the total to obtain the polarization during the poling process as shown. The applied field, 1.97 MV/cm, is the average value for the specimen of thickness 25 μm. Note that only 5 seconds are required to reach 95% of the polarization achieved after 60 seconds for this value of the field. These results are similar to those reported by Southgate [8].

Using the step function polarization process a set of data was obtained at various applied fields. The results are tabulated in Table I and illustrated in Fig. 6, where P_0 is plotted against the applied field, E. The scatter in the data at constant field, in particular at 2 MV/cm, is attributed to the different poling times used and sample variation. (Each point pertains to a different specimen.) The numbers in the left hand column of Table I identify the points in Fig. 6 and other figures appearing later which depict corresponding piezo- and pyroelectric data. According to the data of Fig. 6, a threshold field of about 1 MV/cm is necessary before significant values of P_0 are obtained. Below this value the response (P versus E) is reversible as indicated by single valued response curves observed at low fields.

According to the theory of Broadhurst and co-workers [2] the piezo- and pyroelectric coefficients are linear functions of the remnant polarization. These coefficients, d_p and p_y are plotted with respect to P_0 in Figs. 7 and 8, respectively, and tabulated in Table I. The solid lines illustrate the predictions for no countercharge and for full countercharge as indicated. The values lie nearer to the no-countercharge prediction, possibly indicating a lack of sufficient countercharge to build up a significant moment opposite that due to dipoles. Data of Southgate [8] for similar PVDF films of different thickness and poled by corona discharge

are included in Fig. 8. Southgate's data give smaller values of p_y than ours, especially at higher polarization. Experimental and calculated linear coefficients are given in Table II, which shows that the data support the predictions made without including countercharge and within the stated uncertainties. The apparent leveling-off of Southgate's p_y values at higher polarizations is not predicted by the theory and may reflect errors in polarization due to accumulation of conduction charges at high poling fields, where the conductance is non-ohmic, and, from observations in our laboratory, increases with time prior to breakdown of the specimen.

Both the piezo- and pyroelectric coefficients are determined with a single specimen loading using the same apparatus [23]. The only distinction in the procedure is in the application of changes in the independent variables, temperature and pressure. For this reason, along with the fact that these coefficients appear to be nearly proportional to the remnant polarization it is reasonable to assume that the influence of possible systematic errors, in particular in the measurement of polarization, will be reduced when plotting one of these coefficients with respect to the other.

The results of the comparison between d_p and p_y are presented in Fig. 9, where d_p is plotted against p_y, and the results of the data fit are given in Table II. The theoretical line is determined from Eqs (2), using the average of the results for $\kappa = 1$ and $\kappa = 0$. The influence of countercharge is suppressed in this manner of presentation because the slope of .507 K/MPa differs by only 0.2% for the two extreme cases. The experimental line is taken from a linear least square fit on the data in Table I shown as solid circles in Fig. 8. In this case the fit on the data is constrained to the condition that the curve pass through the origin, since inactive specimens gave no detectable response to either temperature or pressure changes and represented data at 0, 0 having a very small uncertainty. Although the agreement between theory and experiment seems to be improved with this presentation, the theoretical slope of 0.50 K/MPa is 13% higher than the experimental one, 0.44.

CONCLUSIONS

Polyvinylidene fluoride can be given a permanent polarization by application of D.C. electric fields greater than 1 MN/cm for a few seconds. A plasma of air at appropriately low pressures makes an effective electrode for this purpose. The resulting specimens have polarizations and piezoelectric and pyroelectric coefficients which are consistent with a model of aligned polar crystals which change polarization mainly under the influence of thermally and mechanically induced stress.

ACKNOWLEDGMENTS

The authors are indebted to Dr. P. D. Southgate of RCA Laboratories for supplying us his data in tabulated form and to Mr. Steven Roth of our laboratories for his assistance in sample preparation and instrumentation. We also gratefully acknowledge financial support from the Office of Naval Research.

REFERENCES

1. G. T. Davis, J. E. McKinney, M. G. Broadhurst, and S. C. Roth, J. Appl. Phys. 49, 4998 (1978).

2. M. G. Broadhurst, G. T. Davis, J. E. McKinney, R. E. Collins, J. Appl. Phys. 49, 4992 (1978).

3. J. E. McKinney and G. T. Davis, Organic Coatings Plastics, Chem. 38, 271 (1978). (preprints for ACS meeting in Anaheim, Calif., 1978).

4. G. W. Day, C. A. Hamilton, R. L. Peterson, R. J. Phelan Jr. and L. O. Mullen, Appl. Phys. Letters 24, 456 (1974).

5. M. G. Broadhurst, G. T. Davis, S. C. Roth and R. E. Collins, 1976 Annual Report Conference on Electrical Insulation and Dielectric Phenomena, National Academy of Sciences, p. 38 (1978).

6. S. Hunklinger, H. Sussner and K. Dransfeld, in Advances in Solid State Physics, J. Treusch, Ed., Vieweg, Braunschweig, 1976, Vol. XVI, p. 267.

7. H. Sussner, and K. Dransfeld, J. Polymer Science, Polymer Physics ed, 16, 529 (1978).

8. P. D. Southgate, Appl. Phys. Letter. 28, 250 (1976).

9. W. R. Blevin, Appl. Phys. Letter 31, 6 (1977).

10. M. Tamura, S. Hagiwara, S. Matsumoto, and N. Ono, J. Appl. Phys. 48, 513, (1977).

11. R. G. Kepler, Organic Coatings Plast. Chem 38, 278 (1978). (Preprints for ASC Meeting in Anaheim Calif., March 1978).

12. M. Oshiki and E. Fukada, J. Mater. Sci. 10, 1, (1975).

13. N. Murayama, T. Oikawa, T. Katto and K. Nakamura, J. Polymer Science, Polymer Physics ed. 13, 1033 (1975).

14. J. P. Luongo, J. Polymer Science A-2, 10, 1119 (1972).

15. D. Naegele, D. Y. Yoon and M. G. Broadhurst, Macromolecules, 11, 1297, (1978).

16. E. Fukada, M. Date and T. Furukawa, Organic Coatings Plast. Chem 38, 262 (1978). (Preprints for ACS Meeting in Anaheim, Calif., 1978).

17. M. Latour, Polymer, 18, 278 (1977).

18. D. Naegele and D. Y. Yoon, Appl. Phys. Letter 33, 132, (1978).

19. R. G. Kepler and R. A. Anderson, J. Appl. Phys. 49 (1978).

20. D. K. DasGupta and K. Doughty, Appl. Phys. Lett. 31, 585 (1977).

21. G. R. Davies and H. Singh, Submitted to Polymer

22. N. Takahashi and A. Odajima, Extended Abstracts, International Workshop on Electric Charges in Dielectrics, Kyoto, Japan p.88 (1978).

23. M. G. Broadhurst, C. G. Malmberg, F. I. Mopsik, and W. P. Harris, in Electrets, Charge Storage and Transport in Dielectrics, M. M. Perlman, ed. The Electrochemical Soc. Princeton, N.J. p.492 (1973).

24. B. A. Newman, C. H. Yoon, and K. D. Pae, Technical Reports, Number 11 (1977) and 13 (1978) for the Office of Naval Research under Task Number NR 356-564.

TABLE I

Summary of

Experimental Data

Point Number	V_p kV	E MV/cm	P_o $\mu C/cm^2$	d_p pC/N^2	p_y $nC/cm^2\ K$
1	3	1.18	0.59	0.52	____
2	4	1.57	2.49	6.2	1.47
3	5	1.97	3.72	8.4	2.02
4	5	1.97	4.05	6.7	1.61
5	5	1.97	5.06	10.4	2.45
6	5	1.97	5.48	11.2	2.44
7	7	2.76	5.98	13.2	2.87
8	6	2.36	6.13	11.6	2.86
9	7	2.76	7.58	14.3	2.90

TABLE II

Results of Fitting data to $y = ax + b$ and Predicted Results

Experimental*

y	x	a	b	Std. Dev. in y
d_p	P_o	$1.96 \pm 0.17(\times 10^{-10})\ m^2N^{-1}Pa^{-1}$	$0.23 \pm 0.87\ pCN^{-1}$	1.0 pC/N
d_p	P_o	$2.00 \pm 0.06(x.0^{-10})\ m^2N^{-1}Pa^{-1}$		0.98 pC/N
p_y	P_o	$0.33 \pm 0.06(\times 10^{-3})K^{-1}$	$0.66 \pm 0.30\ nC\ cm^{-2}K^{-1}$	$0.24\ nCcm^{-2}K^{-1}$
p_y	P_o	$0.45 \pm 0.02(\times 10^{-3})K^{-1}$		$0.30\ nCcm^{-2}K^{-1}$
d_p	p_y	$0.50 \pm 0.05(\times 10^{-6})K\ Pa^{-1}$	$-1.35 \pm 1.24\ pCN^{-1}$	0.79 pC/N
d_p	p_y	$0.44 \pm 0.01(\times 10^{-6})K\ Pa^{-1}$		0.80 pC/N

Values of a Calculated From Theory**

		No Countercharge	Full Countercharge
d_p	P_o	$2.1 \pm 0.6(\times 10^{-10})\ Pa^{-1}$	$1.5 \pm 0.4(\times 10^{-10})\ Pa^{-1}$
p_y	P_o	$0.42 \pm 0.13(\times 10^{-3})\ K^{-1}$	$0.30 \pm 0.09(\times 10^{-2})K^{-1}$
d_p	p_y	$0.50 \pm 0.15(\times 10^{-6})\ K\ Pa^{-1}$	$0.50 \pm 0.15(\times 10^{-6})K\ Pa^{-1}$

*. Ordinary linear regression assuming certainty in x. Uncertainties in coefficients represent their standard deviations. Fits with b = o are forced through 0, 0. Assuming certainty in y gave similar results.

**. Estimated 30% uncertainties are due to approximation in the theory and uncertainties in the data used to evaluate the theoretical expressions.

Figure Captions

Fig. 1: Schematic illustration of ionic mobility after poling and its consequences on polarization and piezo- and pyroelectric coefficients.

Fig. 2: Schematic drawing of poling electrode assembly.

Fig. 3: Schematic diagram of poling and monitoring circuit.

Fig. 4: Hysteresis loop obtained from alternating field.

Fig. 5: Time dependent response to step function field - on and off.

Fig. 6: Values of remnant polarization plotted against poling field for PVDF.

Fig. 7: Piezoelectric coefficient versus polarization. The solid lines are the theoretical predictions for no countercharge and full countercharge.

Fig. 8: Pyroelectric coefficient versus remnant polarization. Open circles - our data. Closed circles - Ref. 8.

Fig. 9: Piezoelectric versus pyroelectric coefficients. The influence of countercharge essentially converges to single values as indicated by the theoretical line. The experimental line is obtained from a linear regression of the data with the intercept fixed at the origin.

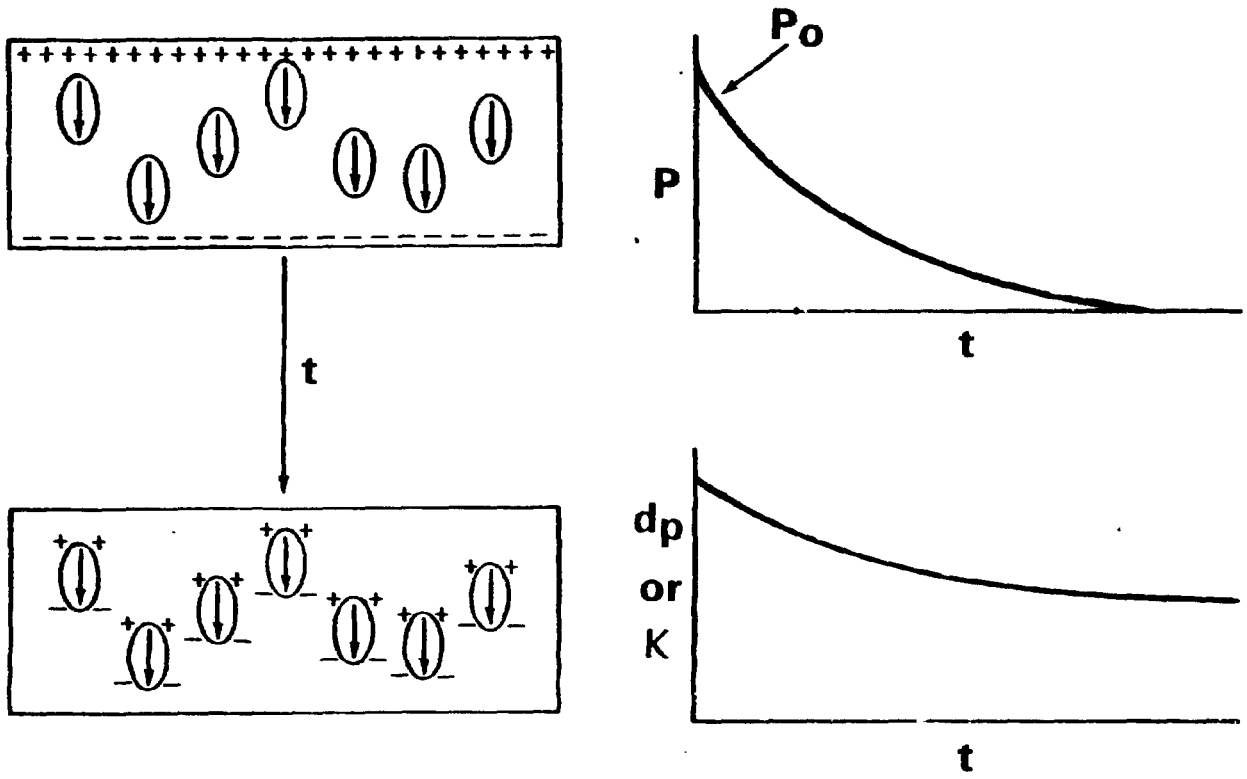

Figure 1

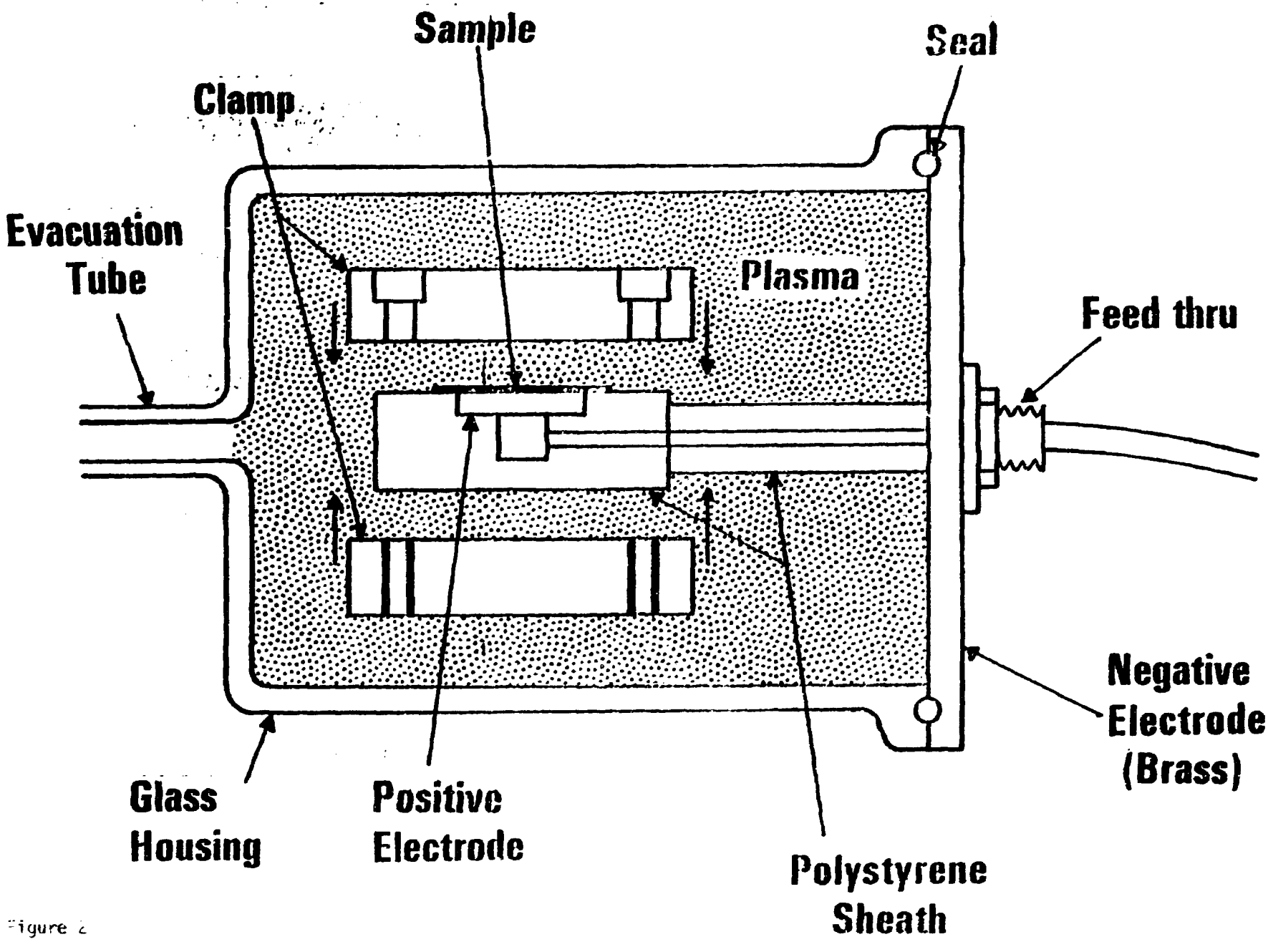
Sample
Seal
Clamp
Evacuation Tube
Plasma
Feed thru
Negative Electrode (Brass)
Glass Housing
Positive Electrode
Polystyrene Sheath

Figure 2

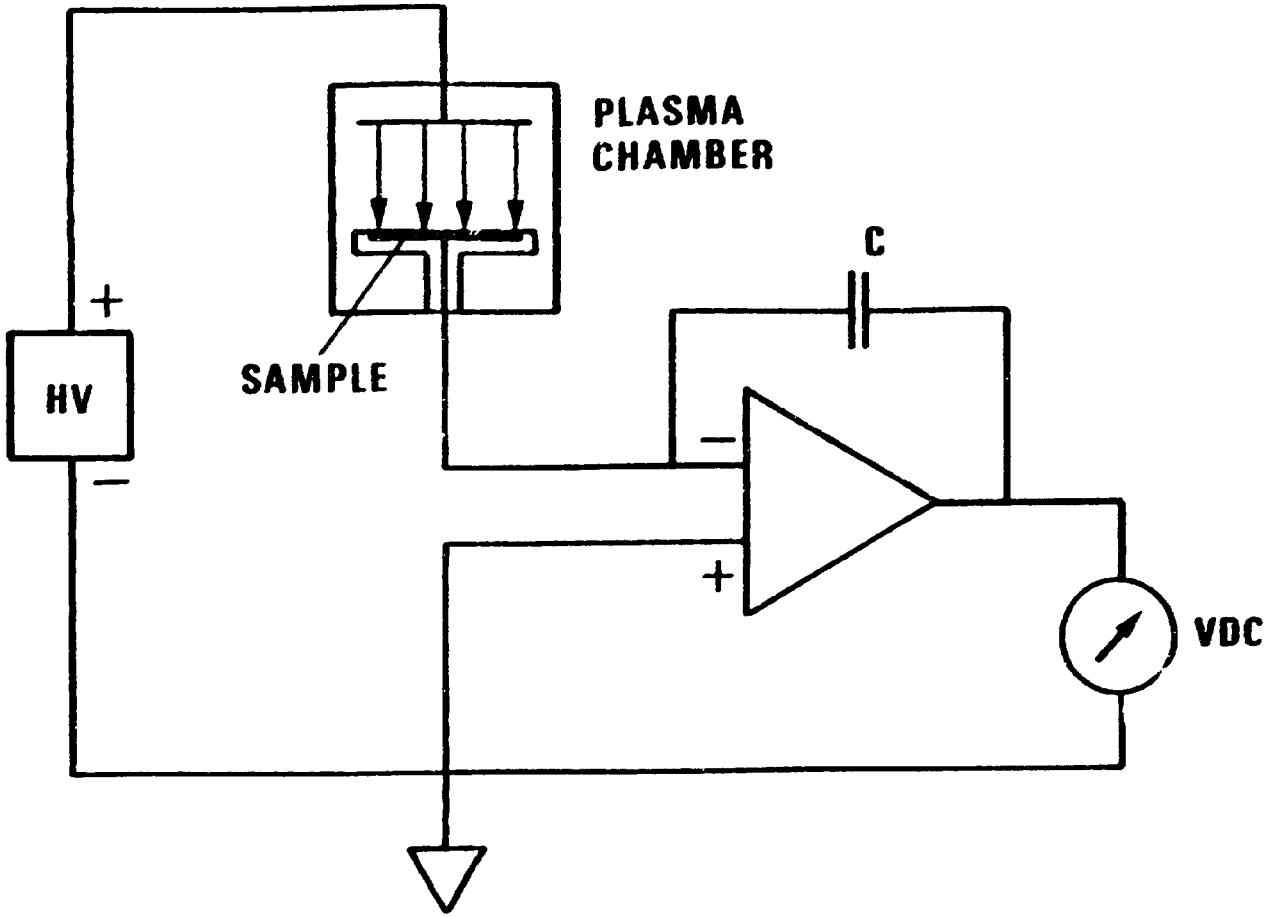

Figure 3

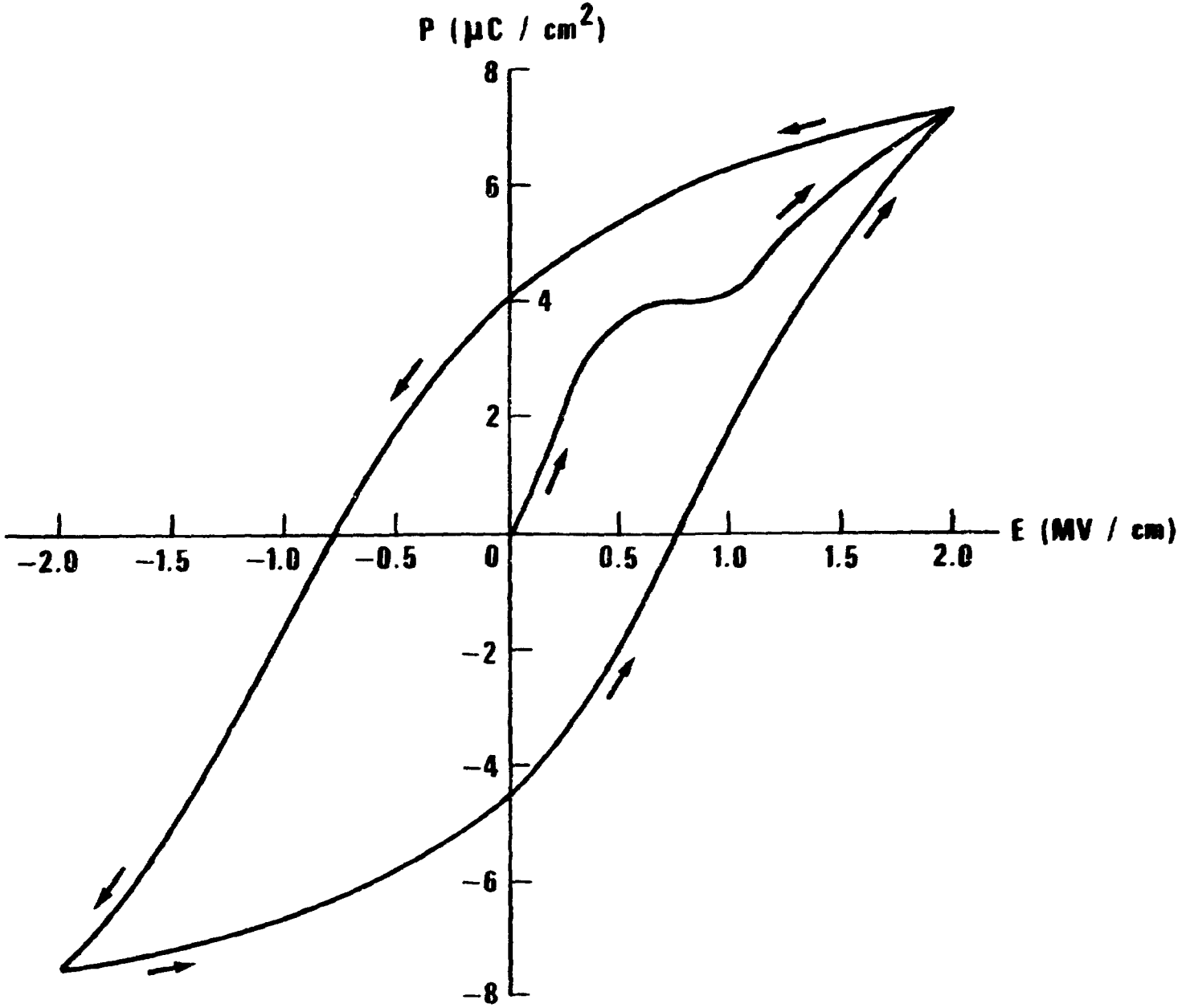

Figure 4

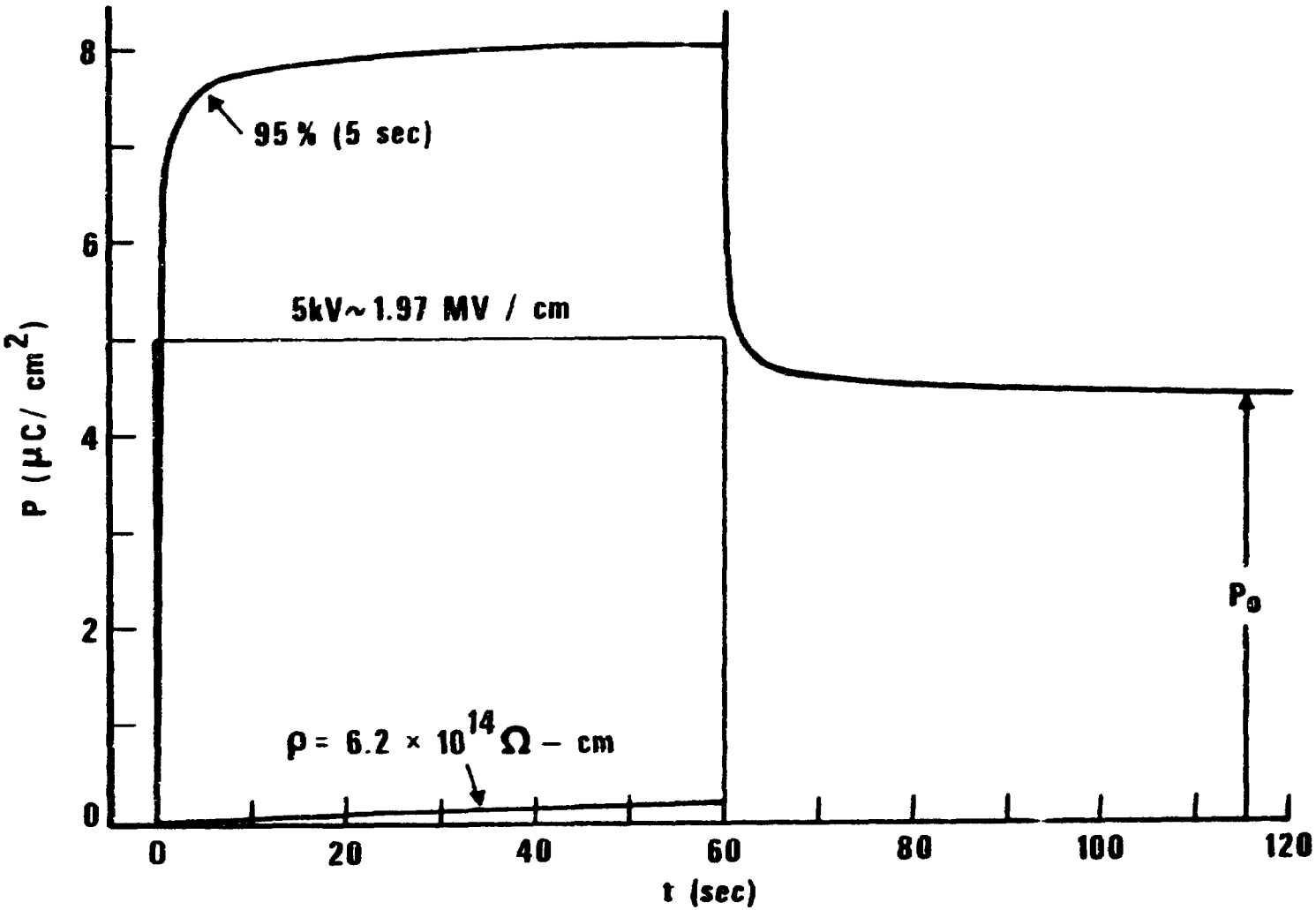
8
6
4
2
0
P (μC/ cm²)
95 % (5 sec)
5kV~ 1.97 MV / cm
ρ = 6.2 × 10¹⁴ Ω – cm
P₀
0
20
40
60
80
100
120
t (sec)

Figure 5

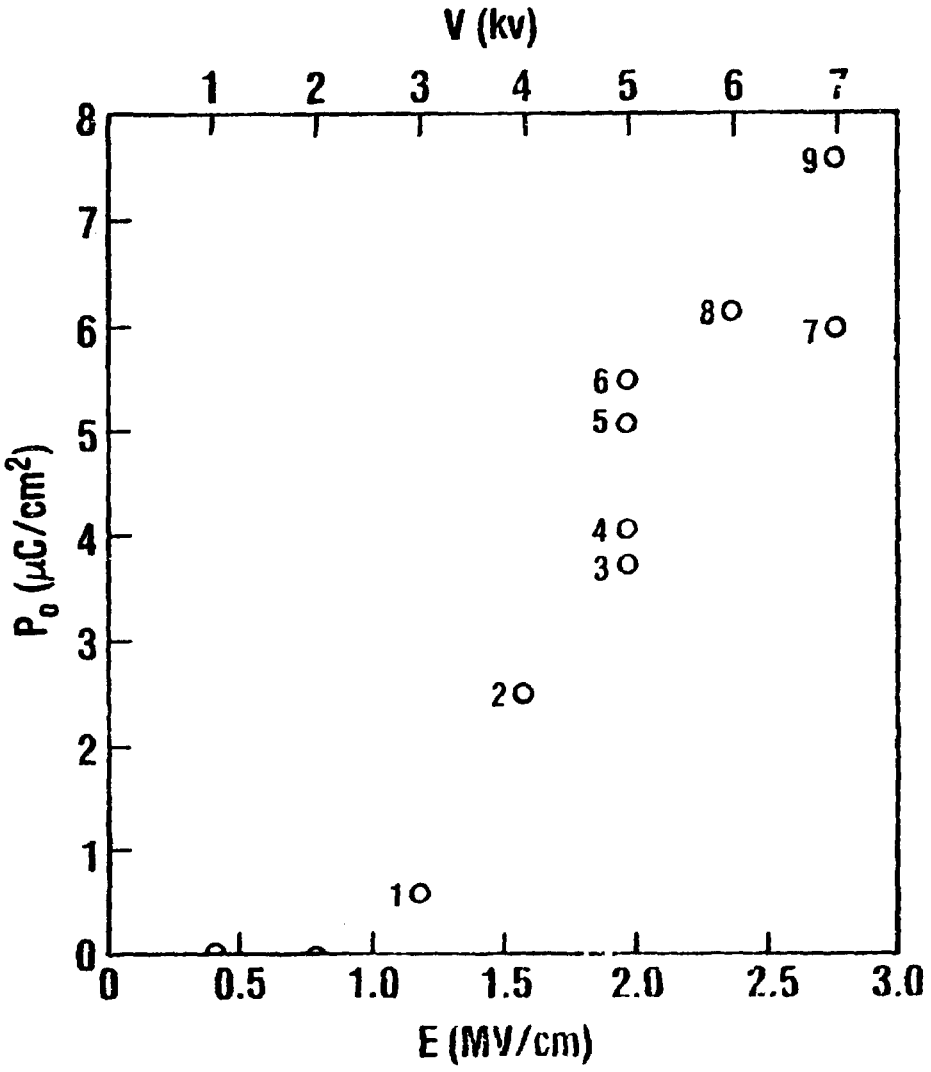
V (kv)
1
2
3
4
5
6
7
8
7
6
5
4
3
2
1
0
P_o ($\mu C/cm^2$)
0
0.5
1.0
1.5
2.0
2.5
3.0
E (MV/cm)
90
80
70
60
50
40
30
20
10

Figure 6

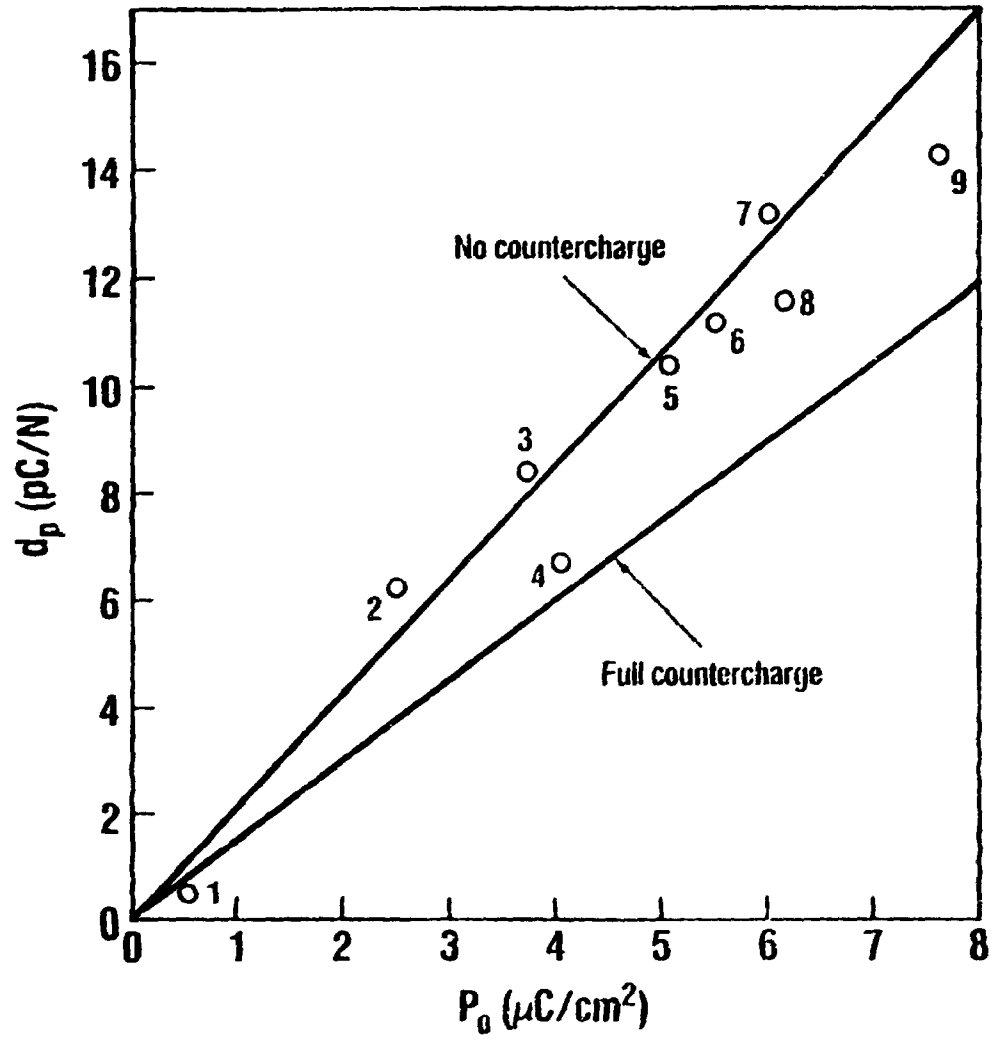
16
14
12
10
8
6
4
2
0
0
1
2
3
4
5
6
7
8
d_p (pC/N)
P_0 (μC/cm^2)
No countercharge
Full countercharge
1
2
3
4
5
6
7
8
9

Figure 7

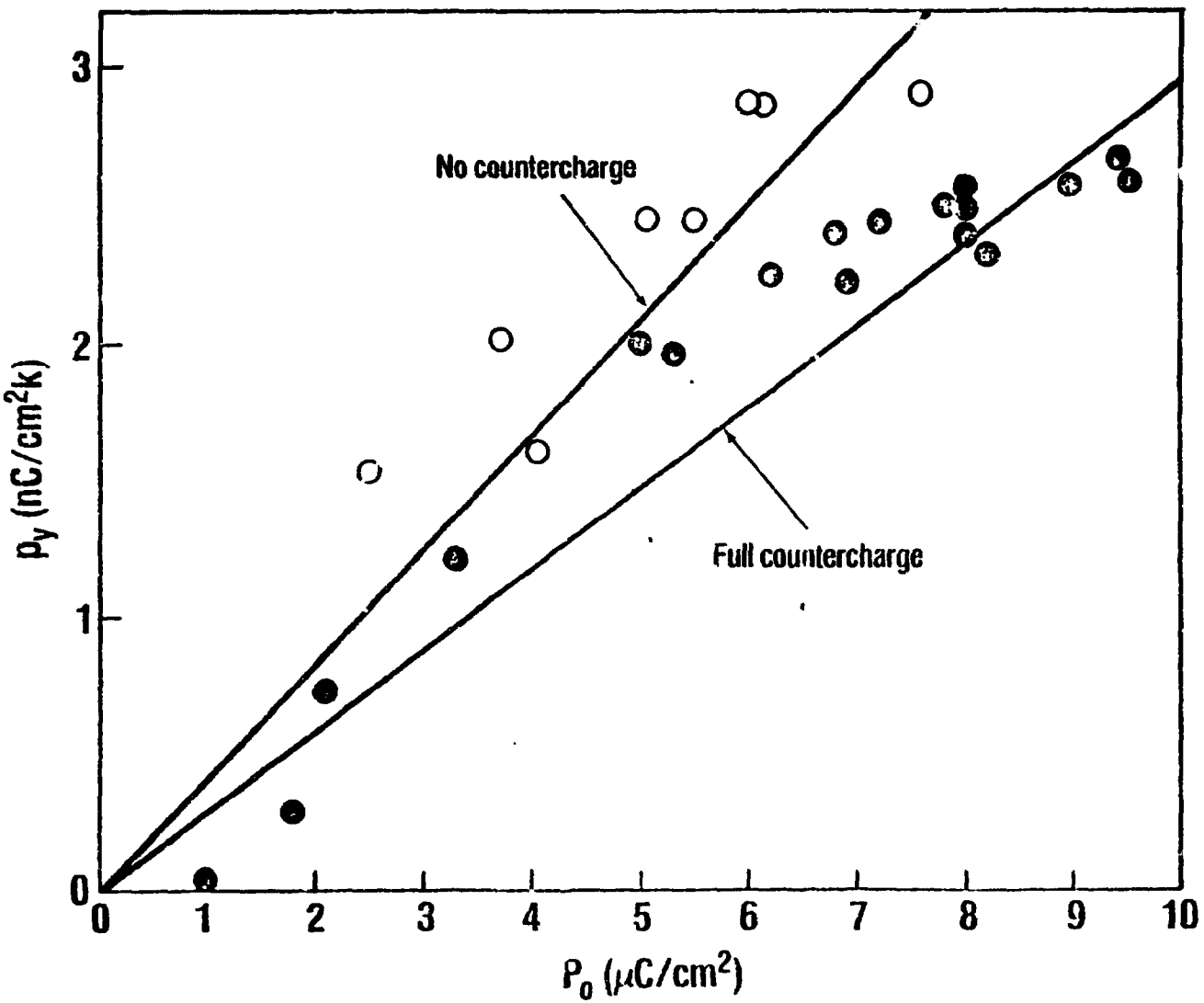
No countercharge
Full countercharge
P_y (nC/cm^{2}k)
P_0 (μC/cm^2)
0
1
2
3
4
5
6
7
8
9
10

Figure 8

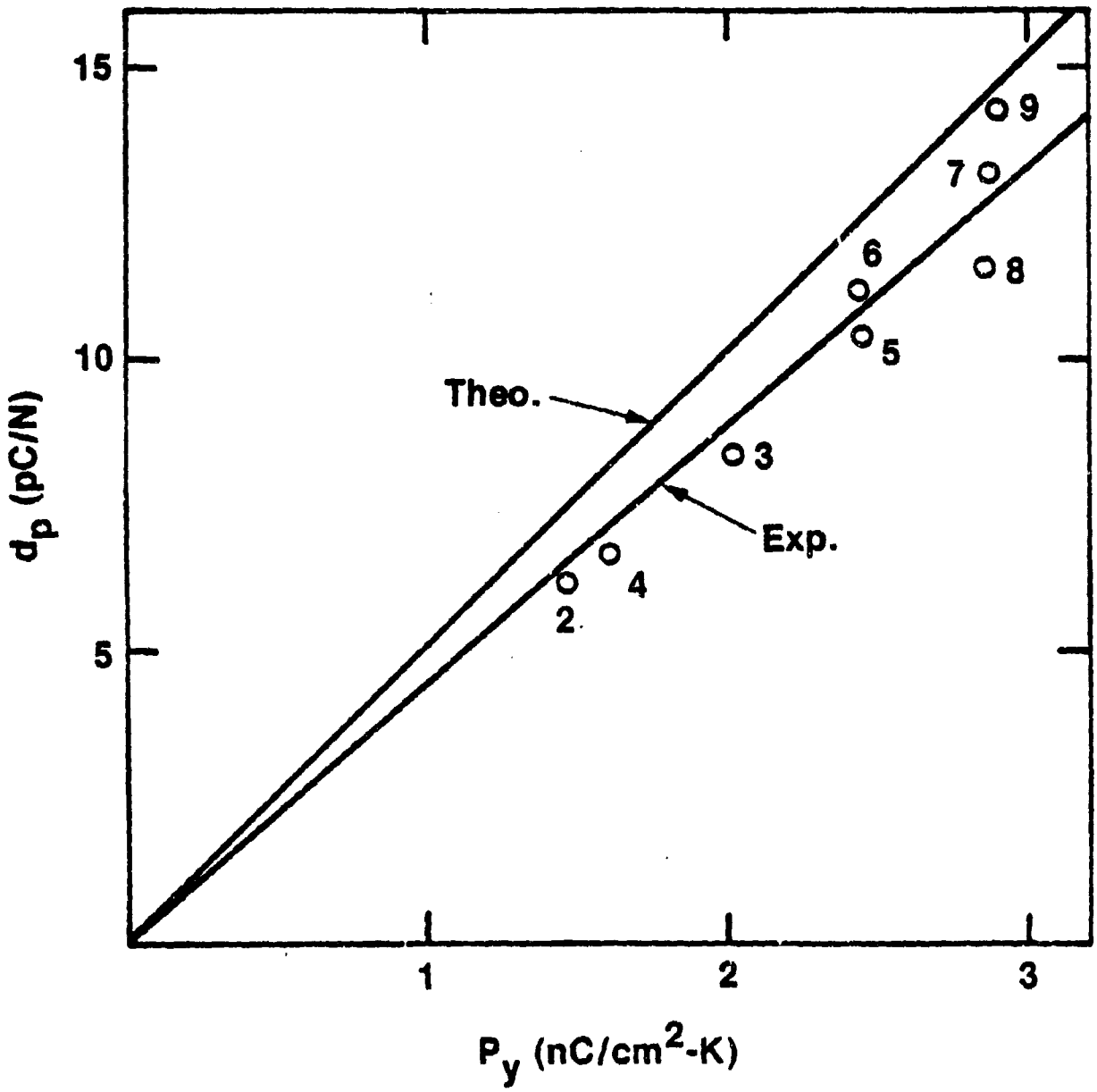

Figure 9

472:GAN:716:tam
78u472-608

TECHNICAL REPORT DISTRIBUTION LIST, GEN

	No. Copies
Office of Naval Research 800 North Quincy Street Arlington, Virginia 22217 Attn: Code 472	2
ONR Branch Office 536 S. Clark Street Chicago, Illinois 60605 Attn: Dr. George Sandos	1
ONR Branch Office 715 Broadway New York, New York 10003 Attn: Scientific Dept.	1
ONR Branch Office 1030 East Green Street Pasadena, California 91106 Attn: Dr. R. J. Marcus	1
ONR Area Office One Hallidie Plaza, Suite 601 San Francisco, California 94102 Attn: Dr. P. A. Miller	1
ONR Branch Office Building 114, Section D 666 Summer Street Boston, Massachusetts 02210 Attn: Dr. L. H. Peebles	1
Director, Naval Research Laboratory Washington, D.C. 20390 Attn: Code 6100	1
The Assistant Secretary of the Navy (R,E&S) Department of the Navy Room 4E736, Pentagon Washington, D.C. 20350	1
Commander, Naval Air Systems Command Department of the Navy Washington, D.C. 20360 Attn: Code 310C (H. Rosenwasser)	1
Defense Documentation Center Building 5, Cameron Station Alexandria, Virginia 22314	12
U.S. Army Research Office P.O. Box 1211 Research Triangle Park, N.C. 27709 Attn: CRD-AA-IP	1
Naval Ocean Systems Center San Diego, California 92152 Attn: Mr. Joe McCartney	1
Naval Weapons Center China Lake, California 93555 Attn: Dr. A. B. Amster Chemistry Division	1
Naval Civil Engineering Laboratory Port Hueneme, California 93401 Attn: Dr. R. W. Drisko	1
Professor K. E. Woehler Department of Physics & Chemistry Naval Postgraduate School Monterey, California 93940	1
Dr. A. L. Slafkosky Scientific Advisor Commandant of the Marine Corps (Code RD-1) Washington, D.C. 20380	1
Office of Naval Research 800 N. Quincy Street Arlington, Virginia 22217 Attn: Dr. Richard S. Miller	1
Naval Ship Research and Development Center Annapolis, Maryland 21401 Attn: Dr. G. Bosmajian Applied Chemistry Division	1
Naval Ocean Systems Center San Diego, California 91232 Attn: Dr. S. Yamamoto, Marine Sciences Division	1

Encl 1

472:GAN:716:tam
78u472-608

TECHNICAL REPORT DISTRIBUTION LIST, 356A

	No. Copies
Dr. Stephen H. Carr Department of Materials Science Northwestern University Evanston, Illinois 60201	1
Dr. M. Broadhurst Bulk Properties Section National Bureau of Standards U.S. Department of Commerce Washington, D.C. 20234	2
Dr. T. A. Litovitz Department of Physics Catholic University of America Washington, D.C. 20017	1
Dr. R. V. Subramanian Washington State University Department of Materials Science Pullman, Washington 99163	1
Dr. M. Shen Department of Chemical Engineering University of California Berkeley, California 94720	1
Dr. V. Stannett Department of Chemical Engineering North Carolina State University Raleigh, North Carolina 27607	1
Dr. D. R. Uhlmann Department of Metallurgy and Material Science Center for Materials Science and Engineering Massachusetts Institute of Technology Cambridge, Massachusetts 02139	1
Naval Surface Weapons Center White Oak Silver Spring, Maryland 20910 Attn: Dr. J. M. Augl Dr. B. Hartman	1
Dr. G. Goodman Globe Union Incorporated 5757 North Green Bay Avenue Milwaukee, Wisconsin 53201	1
Picatinny Arsenal SMUPA-FR-M-D Dover, New Jersey 07801 Attn: A. M. Anzalone Building 3401	1
Dr. J. K. Gillham Princeton University Department of Chemistry Princeton, New Jersey 08540	1
Douglas Aircraft Co. 3855 Lakewood Boulevard Long Beach, California 90846 Attn: Technical Library Cl 290/36-84 AUTO-Sutton	1
Dr. E. Baer Department of Macromolecular Science Case Western Reserve University Cleveland, Ohio 44106	1
Dr. K. D. Pae Department of Mechanics and Materials Science Rutgers University New Brunswick, New Jersey 08903	1
NASA-Lewis Research Center 21000 Brookpark Road Cleveland, Ohio 44135 Attn: Dr. T. T. Serofini, MS-49-1	1
Dr. Charles H. Sherman, Code TD 121 Naval [illegible]rwater Systems Center New Lo[illegible] Connecticut	1
Dr. William Risen Department of Chemistry Brown University Providence, Rhode Island 02192	1
Dr. Alan Gent Department of Physics University of Akron Akron, Ohio 44304	1

472:GAN:716:tam
78u472-608

TECHNICAL REPORT DISTRIBUTION LIST, 356A

	No. Copies
Mr. Robert W. Jones Advanced Projects Manager Hughes Aircraft Company Mail Station D 132 Culver City, California 90230	1
Dr. C. Giori IIT Research Institute 10 West 35 Street Chicago, Illinois 60616	1
Dr. M. Litt Department of Macromolecular Science Case Western Reserve University Cleveland, Ohio 44106	1
Dr. R. S. Roe Dopartment of of Materials Science anc Metallurgical Engineering University of Cincinnati Cincinnati, Ohio 45221	1
Dr. L. E. Smith U.S. Department of Commerce National Bureau of Standards Stability and Standards Washington, D.C. 20234	1
Dr. Robert E. Cohen Chemical Engineering Department Massachusetts Institute of Technology Cambridge, Massachusetts 02139	1
Dr. David Roylance Department of Materials Science and Engineering Massachusetts Institute of Technology Cambridge, Massachusetts 02039	1
Dr. T. P. Conlon, Jr., Code 3622 Sandia Laboratories Sandia Corporation Albuquerque, New Mexico	1
Dr. Martin Kaufmann, Head Materials Research Branch, Code 4542 Naval Weapons Center China Lake, California 93555	1
Dr. T. J. Reinhart, Jr., Chief Composite and Fibrous Materials Branch Nonmetallic Materials Division Department of the Air Force Air Force Materials Laboratory (AFSC) Wright-Patterson Air Force Base, Ohio 4543	1
Dr. J. Lando Department of Macromolecular Science Case Western Reserve University Cleveland, Ohio 44106	
Dr. J. White Chemical and Metallurgical Engineering University of Tennessee Knoxville, Tennessee 37916	1
Dr. J. A. Manson Materials Research Center Lehigh University Bethlehem, Pennsylvania 18015	1
Dr. R. F. Helmreich Contract RD&E Dow Chemical Co. Midland, Michigan 48640	1
Dr. R. S. Porter University of Massachusetts Department of Polymer Science and Engineering Amherst, Massachusetts 01002	1
Professor Garth Wilkes Department of Chemical Engineering Virginia Polytechnic Institute and State University Blacksburg, Virginia 24061	1
Dr. Kurt Baum Fluorochem Inc. 6233 North Irwindale Avenue Azuza, California 91702	1
Professor C. S. Paik Sung Department of Materials Sciences and Engineering Massachusetts Institute of Technology Cambridge, Massachusetts 02139	1